Rotational Spectrum and Internal Dynamics of Tetrahydrofuran–Krypton

ARTICLE *in* CHEMPHYSCHEM · JANUARY 2012

Impact Factor: 3.42 · DOI: 10.1002/cphc.201100673 · Source: PubMed

7 AUTHORS, INCLUDING:

Qian Gou
Chongqing University
40 PUBLICATIONS **160** CITATIONS
SEE PROFILE

Gang Feng
Chongqing University
53 PUBLICATIONS **229** CITATIONS
SEE PROFILE

Luca Evangelisti
University of Bologna
66 PUBLICATIONS **389** CITATIONS
SEE PROFILE

Assimo Maris
University of Bologna
98 PUBLICATIONS **951** CITATIONS
SEE PROFILE

DOI: 10.1002/cphc.201100673

Rotational Spectrum and Internal Dynamics of Tetrahydrofuran–Krypton

Qian Gou,[a] Gang Feng,[a] Luca Evangelisti,[a] Assimo Maris,[a] Marianna Marchini,[a] Biagio Velino,[b] and Walther Caminati*[a]

The rotational spectrum of the tetrahydrofuran–krypton van der Waals complex has been investigated by pulsed-jet Fourier transform microwave spectroscopy. The spectra of the ^{84}Kr and ^{86}Kr isotopologues have been assigned and the krypton atom is located nearly over the oxygen atom, almost perpendicular to the COC plane. Each rotational transition is split into two component lines due to, according to the observed Coriolis coupling term between the tunneling states, the residual pseudorotational effects of the ring in the complex. The splitting between the two vibrational sublevels is 87.462(2) and 87.062(2) MHz for the ^{84}Kr and ^{86}Kr isotopologues, respectively. These splittings have been used to determine the barrier to inversion, $B_2 = 67$ cm^{-1}. The dissociation energy has been estimated to be 3.7 kJ mol^{-1} from centrifugal distortion effects.

1. Introduction

In recent decades, the high-resolution rotational spectroscopic technique has revealed itself to be particularly efficient in studying the nature of van der Waals interactions that dominate the formation of the molecular complexes of rare gas (RG) atoms with organic molecules. Rotational spectra can give precise information on the large-amplitude motions typical of this kind of adducts,[1] especially in conjunction with the observation of even small vibrational splitting.

Generally, complexes with aromatic molecules have the RG atom firmly linked to one side of the ring and van der Waals motions do not generate observable inversion splittings. This is the case, for example, of complexes of pyridine with all RG atoms, that is, RG = He,[2] Ne,[3] Ar,[4] Kr,[4a] or Xe.[5] Alternatively, when a RG atom is linked to an open-chain molecule, such as, for example, dimethyl ether, all complexes, for RG = Ne,[6] Ar,[7] Kr,[8] and Xe,[9] display rotational transitions characterized by inversion splittings. From centrifugal distortion effects, it has been possible to estimate the dissociation energies of the complexes, which are higher for the aromatic molecules complexes and increase with the atomic number of RG. Tunneling splittings are useful to determine the barrier to inversion along the tunneling motion.

Aliphatic ring organic molecules are intermediate between aromatic molecules and open-chain molecules as far as tunneling splittings are concerned.

THF is a fully aliphatic cyclic nonplanar molecule that undergoes a pseudorotation motion, with a consequent splitting into four pseudorotation substates of the ground vibrational state.[10] The complex of THF with Ar (THF–Ar) displayed a systematic doubling of the rotational lines.[11] According to the observed Coriolis coupling constants, the observed tunneling splitting was mainly attributed to the residual pseudorotation effects of the THF subunit in the complex. To check if the interpretation of the doubling in THF–Ar was correct, to investigate the influence of the RG atomic weight and polarizability on the tunneling effects, and to model the potential energy function of the tunneling motion, we decided to analyze the rotational spectrum of the THF–Kr complex.

2. Results and Discussion

2.1. Theoretical Calculations

Before collecting the rotational spectrum, we performed some theoretical calculations to obtain an insight into the equilibrium conformation of the complex.

THF–Kr is schematically shown in Figure 1, together with the parameters defining the position of the Kr atom used throughout the text. On going from the molecule to the complex, an inversion of the principal axis of inertia takes place with respect to the ring skeleton. The position of Kr in the complex can be described with the spherical coordinates R_{CM}, θ, and ϕ. R_{CM} is the distance of the Kr atom from the center of mass of the monomer, θ is the angle that R_{CM} makes with the *c* principle axis of THF, and ϕ is the angle between the projection of R_{CM} in the *ab* plane and the *a* principle axis of THF.

First we applied the DPM.[12] The calculations were performed by using the computer program RGDMIN with full minimization of the structural van der Waals parameters.[13] This

[a] Q. Gou, G. Feng, Dr. L. Evangelisti, Dr. A. Maris, M. Marchini, Prof. Dr. W. Caminati
Department of Chemistry
University of Bologna
Via Selmi 2
I-40126 Bologna (Italy)
E-mail: walther.caminati@unibo.it

[b] Dr. B. Velino
Department of Physical and Inorganic Chemistry
University of Bologna (Italy)

Supporting information for this article is available on the WWW under http://dx.doi.org/10.1002/cphc.201100673.

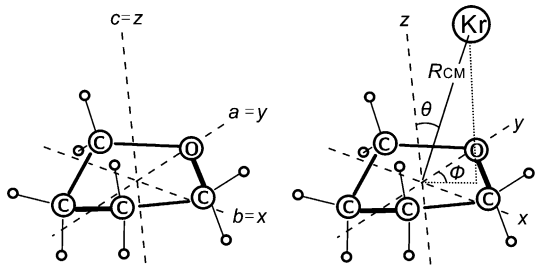

Figure 1. Sketch of THF–Kr. The spherical coordinates locating the position of Kr used in the distributed polarizability model (DPM) calculation are defined. The principal axis of the complex are, in a first approximation, linked to the x, *y*, *z* coordinates according to $x \approx b$, $y \approx c$, $z \approx a$.

method is very simple, fast, and very efficient for finding different possible minima on the van der Waals potential energy surface.[14] Subsequently, we refined the global minimum found with RGDMIN by ab initio calculations at the MP2/6-311++G(d,p) level using the Gaussian 03 program package.[15] The calculated rotational constants and electric dipole moments are listed in Table 1, whereas the three spherical coordinates are given in a subsequent section. According to the calculated electric dipole moment components, we expected to observe an asymmetric rotor spectrum with weak *a*- and *b*-type transitions and stronger *c*-type transitions.

Table 1. Rotational constants and components of the electric dipole moment of THF–Kr calculated by MP2/6-311++G(d, p) and DPM.

	MP2/6-311++G(d, p)	DPM
A [MHz]	4371	4240
B [MHz]	784	755
C [MHz]	773	747
$\lvert\mu_a\rvert$ [D]	0.9	–
$\lvert\mu_b\rvert$ [D]	0.8	–
$\lvert\mu_c\rvert$ [D]	1.5	–

2.2. Rotational Spectrum and Analysis

The spectrum of the most abundant isotopic species (^{84}Kr, ca. 57% of natural abundance) was investigated first. Since THF–Kr has almost a prolate symmetric top, the *S* reduction and I^r representations were chosen.[16] The frequencies were fitted with the Pickett SPFIT computer program,[17] according to the reduced axis Hamiltonian given in Equation (1):

$$H = \sum_i H_i + H_{0^+0^-} \quad (i = 0^+, 0^-) \tag{1}$$

in which H_i is given by Equation (2):

$$H_i = A(i)P_a^2 + B(i)P_b^2 + C(i)P_c^2 - D_J P^4 - D_{JK}P_a^2P^2 + d_1P^2\left(P_+^2 + P_-^2\right) + d_2\left(P_+^4 + P_-^4\right) \tag{2}$$

and $H_{0^+0^-}$ is given by Equation (3):

$$H_{0^+0^-} = [F_{bc} + F'_{bc}J(J+1)](P_bP_c + P_cP_b) + F_{ab}(P_aP_b + P_bP_a) + \Delta E_{0^+0^-} \tag{3}$$

Several μ_a-R-type lines, with *J* values ranging from 5 to 11, were initially assigned and some μ_c-R-type lines were measured. Both μ_a- and μ_c-type lines are split into two nearby components, as shown in Figure 2 for the $6_{1,6} \leftarrow 5_{1,5}$ transition. Below we show that they are intrastate transitions due to a tunneling motion in THF–Kr.

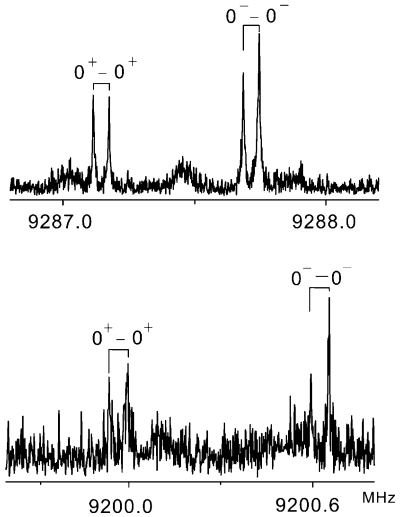

Figure 2. Recorded $6_{1,6} \leftarrow 5_{1,5}$ transitions, split into two tunneling component lines, for the ^{84}Kr (top) and ^{86}Kr (bottom) isotopologues. Each line appears as a doublet ($\prod$) due to the Doppler effect.

The vibration–rotation transitions $5_{1,5}(0^-) \leftarrow 4_{1,3}(0^+)$ and $5_{1,4}(0^+) \leftarrow 4_{1,4}(0^-)$, which were, in principle, forbidden, were observed at 7743.889 ($\nu_{obsd} - \nu_{calcd} = 0.67$ kHz) and 7786.077 MHz ($\nu_{obsd} - \nu_{calcd} = 0.03$ kHz), respectively. These transitions have μ_a-type character due to strong mixing between the pairs of states $5_{1,5}(0^-)$–$5_{1,4}(0^+)$ and $4_{1,4}(0^-)$–$4_{1,3}(0^+)$ induced by Coriolis interactions.

Finally, several interstate μ_b-type transitions, which were fully split by twice the vibrational separation between the 0^+ and 0^- sublevels, were assigned and measured.

The 14 spectroscopic parameters determined are listed in Table 2. There are three rotational constants for each of the coupled states, four quartic centrifugal distortion constants (fit to a common value for the two states), their energy difference ($\Delta E_{0^+0^-}$), the interaction constants F_{ab} and F_{bc}, and *J*-dependence constant F'_{bc}, as defined in the interaction Hamiltonian ($H_{0^+0^-}$).

The spectrum of the second most intense isotopomer (^{86}Kr, ca. 17% of natural abundance) was also measured in the same way. The vibration–rotation transitions $5_{1,5}(0^-) \leftarrow 4_{1,3}(0^+)$ and $5_{1,4}(0^+) \leftarrow 4_{1,4}(0^-)$ at 7671.3488 ($\nu_{obsd} - \nu_{calcd} = -1.50$ kHz) and 7712.2631 MHz ($\nu_{obsd} - \nu_{calcd} = 0.39$ kHz), respectively, were observed likewise.

All measured transitions are given in the Supporting Information.

The F_{ab} coefficient is larger than F_{bc}, although the latter is better determined due to the small energy separation ($\Delta E_{0^+0^-}$), which is of the same order of magnitude of the rotational

Table 2. Experimental spectroscopic constants of THF–Kr (*S* reduction, I^r representation).[a]

	THF–^{84}Kr		THF–^{86}Kr	
	0^+	0^-	0^+	0^-
A [MHz]	4369.442(6)	4369.569(6)	4369.261(1)	4369.385(1)
B [MHz]	784.394(6)	784.387(6)	776.829(1)	776.821(1)
C [MHz]	773.3362(3)	773.3173(2)	766.0845(2)	766.0604(2)
D_J [kHz]	1.4044(4)		1.3799(9)	
D_{JK} [kHz]	4.46(1)		4.24(6)	
d_1 [kHz]	0.120(2)		[0.120]	
d_2 [Hz]	0.4(1)		[0.4]	
$\Delta E_{0^+0^-}$ [MHz]	87.462(2)		87.070(2)	
F_{ab} [MHz]	127.01(9)		124.57(9)	
F_{bc} [MHz]	−4.3642(2)		−4.2789(1)	
F'_{bc} [kHz]	0.172(4)		[0.172]	
N[b]	60		36	
σ[c] [kHz]	1.10		1.60	

[a] The error in the last digit is given in parentheses. Values in square brackets are fixed at the values for THF–^{84}Kr. [b] Number of transitions in the fit. [c] Standard deviation of the fit.

Table 3. Experimental (r_s and r_0) and theoretical (r_e and r_{DPM}) van der Waals structural parameters of THF–^{84}Kr.[a]

	r_0	r_s	r_e	r_{DPM}
Kr coordinates in the principal axes system of THF···Kr				
$\lvert a \rvert$ [Å]	1.774	1.766(1)	1.775	1.812
$\lvert b \rvert$ [Å]	0.004	0.13(1)	0.004	0.003
$\lvert c \rvert$ [Å]	0.067	0.0[b]	0.067	0.060
Kr coordinates in the principal axes system of THF				
$\lvert a \rvert$ [Å]	1.377	1.62(1)	1.430	1.245
$\lvert b \rvert$ [Å]	0.750	0.2(1)	0.652	0.668
$\lvert c \rvert$ [Å]	3.508	3.488(1)	3.508	3.661
Kr van der Waals parameters				
R_{CM} [Å]	3.843(1)	3.841	3.845	3.924
θ [°]	24.1(1)	24.8	24.1	21.1
ϕ [°]	29(4)	5.7	24.5	28.2

[a] Errors in the last digit are given in parentheses. [b] An imaginary value that is set to zero.

spacing between many of the observed K_a asymmetry doublets. These data help to understand what kind of motion is responsible for the tunneling splitting, which evidently indicates a double minimum potential owning to a large amplitude motion of the complex. This motion could be 1) the residual pseudorotation of the ring in the complex, or 2) the transfer of Kr from above to below the THF ring (see Figure 1). In the first case, the angular momentum vector oriented along the *a* axis of isolated THF should have components mainly along *a* and *c* axes of THF–Kr. Orienting along the *a* axis of THF, a larger projection along the *c* axis than the *a* axis of THF–Kr is expected. As in the principle inertial axes system, Coriolis coupling could be interpreted in terms of the angular momentum operator.[17a] This is in good agreement with the fact that the *a*- and *c*-type coupling terms, F_{bc} and F_{ab}, are observed between the tunneling states of THF–Kr; the *c*-type coupling is larger. In addition, the μ_b dipole moment component should invert when going from one minimum to the equivalent one, and correspondingly μ_b-type transitions should be interstate transitions. In contrast, in the second case, μ_c-type transitions should be the interstate ones. Therefore, the kinds of observed Coriolis coupling terms and interstate transitions allow us to conclude that the observed tunneling splitting should be in connection with a residual pseudorotation of the THF subunit. Similar behavior has also been observed for some hydrogen-bonded complexes involving THF, such as THF···HCl[18] and THF···HF,[19] the rotational spectra of which present doublets owing to pseudorotational tunneling of THF.

2.3. Location of the Kr Atom in the Complex

Four different sets (r_0, r_s, r_{DPM}, and r_e) of van der Waals structural parameters of the complex are shown in Table 3.

The partial r_0 structure was obtained by fitting the distance R_{CM} and the angles θ and ϕ, indicated in Figure 1, to the available rotational constants, starting from the ab initio structure. The r_s coordinates[20] of the krypton atom can be obtained in the principal axes system of THF by a hypothetical substitution of an atom of zero mass with Kr on going from THF to THF–Kr, or in the principal axes system of THF–^{84}Kr when substituting ^{84}Kr with ^{86}Kr. However, these values are approximate because of van der Waals vibrations, which take place only in the complex. The r_e and r_{DPM} geometries are those obtained by ab initio and DPM calculations, respectively.

The r_0 values are very similar to those of r_e, which means that only a slight adjustment of the van der Waals parameters was required.

2.4. van der Waals Vibrations

2.4.1. van der Waals Stretching

Upon complexation with THF, the three translational degrees of freedom of the isolated krypton atom are replaced by three van der Waals vibrational modes: THF–Kr stretching and two bending modes.

First, we assumed that the Kr stretching motion could be isolated from the other motions. Therefore, the stretching force constant (k_s) was estimated by approximating the complex to a molecule made of two rigid parts. In the presence of several symmetry elements, Millen[21] and Read et al.[22] derived Equation (4) for asymmetric top complexes in which the stretching coordinates are almost parallel to the inertial *a*-axis:

$$k_s = 16\pi^4(\mu_D R_{CM})^2[4B^4+4C^4-(B-C)^2(B+C)^2]/(hD_J) \qquad (4)$$

in which μ_D is the pseudo-diatomic reduced mass, R_{CM} is the distance between the centers of the mass of the monomers, and D_J is the centrifugal distortion constant. After analysis of the spectrum with the Hamiltonian given by Equation (1), D_J should not be contaminated by ring pseudorotation contributions. For THF–Kr, we obtained $k_s = 3.0\ \mathrm{N\,m^{-1}}$, and corresponding to a harmonic stretching fundamental $\nu_k = 36\ \mathrm{cm^{-1}}$.

By assuming a Lennard-Jones potential function, the dissociation energy has been estimated to be 3.7 kJ mol^{-1} by using Equation (5):[23]

$$E_B = k_s R_{CM}^2/72 \quad (5)$$

The dissociation energy of THF–Kr is higher than that of THF-Ar (E_B = 2.6 kJ mol^{-1}),[11] which is in agreement with the higher polarizability of Kr with respect to Ar. The same parameters of complexes involving THF, 2,5-dihydrofuran, pyridine and oxirane with Kr are listed in Table 4.

Table 4. Force constants and dissociation energies of the van der Waals stretching in some complexes of Kr with ring molecules.

	k_s [N m^{-1}]	E_B [kJ mol^{-1}]	Ref.
THF–Kr	3.02	3.7	present work
2,5-dihydrofuran–Kr	3.26	3.5	[24]
pyridine–Kr	3.51	3.8	[4a]
oxirane–Kr	2.69	3.1	[25]

2.5. Tunneling Motion Described by One-Dimensional Flexible Model Calculations

Meyer's one-dimensional flexible model[26] has been used to determine the potential energy barrier between the two equivalent minima due to the up and down bending motions of C5 and C6 with respect to the C3–D2–C4 plane shown in Figure 3. In Figure 3, the notation D refers to "dummy" atoms, which are reference points in the molecule not corresponding to real atoms. This model allows the numerical calculation of rotational and vibrational wave functions and eigenvalues (and then the vibrational spacings), but needs a description of the pathway and a potential energy function. For this purpose, the geometry of the transient states of THF–Ar were obtained from ab initio calculations at the MP2/6-311++G(d,p) level with the Gaussian 03 package; this is given in Table S4 in the Supporting Information.

The experimental value for the barrier was obtained from the $\Delta E_{0^+0^-}$ splitting (see Table 2). The following potential energy function [Eq. (6)] has been adopted:

$$V(\alpha) = B_2[1-(\alpha/\alpha_e)^2]^2 \quad (6)$$

in which the inversion coordinate α is the twisting angle (with respect to the planarity of the four carbon atoms) of the C5 and C6 atoms (see Figure 3). B_2 is the barrier to inversion and α_e is the equilibrium value of the inversion angle. The main relaxations of other structural parameters have been accounted for according to Equation (7) for symmetric variations with respect to α (most parameters):

$$S(\alpha) = S_0 + \Delta S(\alpha/\alpha_e)^2 \quad (7)$$

or according to Equation (8) for asymmetric changes:

$$A(\alpha) = A_0 + \Delta A(\alpha/\alpha_e) \quad (8)$$

For a given parameter S (or A), S_0 (or A_0) is the value at α = 0, while ΔS (or ΔA) is its variation in going from α = 0 to α_e. All of these values were obtained from the ab initio geometries of the minimum and transition state (see Tables S3 and S4 in the Supporting Information).

The results of the flexible model calculations are shown in Table 5. α_0 was fixed at the ab initio value, 25.3°, because there were not enough data to fit this parameter.

The determined potential energy function is shown in Figure 4. The B_2 value, 67 cm^{-1}, is about the double of that suggested by ab initio calculations (34 cm^{-1}). The excellent reproduction of the shift of $\Delta E_{0^+0^-}$ when going from THF–^{84}Kr to THF–^{86}Kr justifies the reliability of the flexible model.

In the flexible model calculations, the α coordinate was considered in the ±50° range and solved into 61 mesh points.[26]

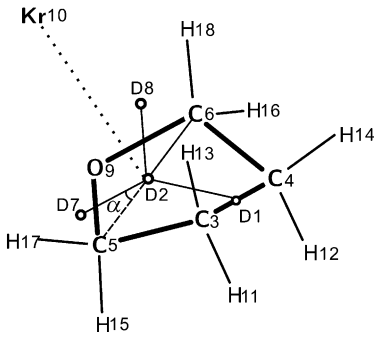

Figure 3. Ring puckering in THF–Kr. α denotes the inversion angle of C5 or C6. D_i (i = 1, 2, 7, or 8) denotes dummy points.

3. Conclusions

The rotational spectrum of THF–Kr was investigated by pulsed-jet Fourier transform microwave spectroscopic techniques. Systematic doubling of the rotational lines was attributed to the

Table 5. Results of the flexible model calculations.

1) Tunneling Splittings	Obsd	Calcd
$\Delta E_{0^+0^-}$ (^{84}Kr)/MHz	87.462(2)[a]	87.51
$\Delta E_{0^+0^-}$ (^{86}Kr)/MHz	87.070(2)[a]	87.12
2) Determined parameters		
B_2 = 67(1) cm^{-1}		α_0 = 25.3°[b]
3) Structural relaxation parameters		
$\Delta S(r_{C5-C6})$ = 0.090 Å	$\Delta S(r_{D1-D2})$ = −0.085 Å	$\Delta S(r_{O9-D2})$ = −0.084 Å
$\Delta S(r_{Kr-D2})$ = −0.192 Å	$\Delta S(_{O9D2D7})$ = 40.8°	$\Delta S(_{KrD2D1})$ = 27.1°
$\Delta A(_{O9D2-D7D8})$ = 0.1°	$\Delta A(_{KrD2-D1C5})$ = 3.4°	$\Delta A(_{H11C3-C5D2})$ = 27.5°[c]

[a] The error in the last digit is given in parentheses. [b] Fixed at the ab initio values. [c] The structural relaxation for the dihedral angle H11C3–C5D2 holds also for the corresponding dihedral angles of H12, H13, H14.

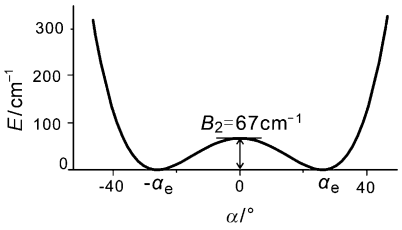

Figure 4. Pseudorotation potential energy function in THF–Kr according to flexible model analysis.

residual pseudorotation of THF in the complex, based on the values of the Coriolis coupling constants and on the type (μ_b) of interstate transitions. Meyer's one-dimensional flexible model analysis proved the potential energy function for the pseudorotation motion.

The strength of the Kr–THF "chemical" bond ($\approx$3.7 kJ mol^{-1}) was higher than that of the related Ar–THF complex, in accordance with the higher polarizability of krypton.

Experimental Section

Molecular clusters were generated in a supersonic expansion under conditions optimized for dimer formation. Details of the Fourier transform MW[27] spectrometer (COBRA-type),[28] which covers the range 6.5–18 GHz, have been described previously.[9b] A gas mixture of about 11% Kr in He at a stagnation pressure of about 0.25 MPa was passed over a sample of THF (commercial sample bought from Aldrich and used without further purification) and expanded through a solenoid valve (General Valve, Series 9, nozzle diameter 0.5 mm) into the Fabry–Pérot cavity. The spectral line positions were determined after Fourier transformation of the time-domain signal with 8 k data points, recorded with 100 ns sample intervals. Each rotational transition appears as a doublet due to the Doppler effect. The line position is calculated as the arithmetic mean of the frequencies of the Doppler components. The estimated accuracy of the frequency measurements is better than 3 kHz. Lines separated by more than 7 kHz are resolvable.

Acknowledgements

We thank Italian MIUR (PRIN08, project KJX4SN_001) and the University of Bologna (RFO) for financial support. G.F. and Q.G. also thank the China Scholarships Council (CSC) for financial support.

Keywords: ab initio calculations · krypton · microwave spectroscopy · tetrahydrofuran · noncovalent interactions

[1] W. Caminati, J.-U. Grabow, *Microwave Spectroscopy: Molecular Systems in Frontiers of Molecular Spectroscopy* (Ed.: J. Laane), Elsevier, **2009**, Chapter 15.
[2] C. Tanjaroon, W. Jäger, *J. Chem. Phys.* **2007**, *127*, 034302.
[3] a) A. Maris, W. Caminati, P. G. Favero, *Chem. Commun.* **1998**, 2625; b) B. Velino, W. Caminati, *J. Mol. Spectrosc.* **2008**, *251*, 176.
[4] a) T. D. Klots, T. Emilsson, R. S. Ruoff, H. S. Gutowsky, *J. Phys. Chem.* **1989**, *93*, 1255; b) R. M. Spycher, D. Petitprez, F. L. Bettens, A. Bauder, *J. Phys. Chem.* **1994**, *98*, 11863; c) S. Melandri, G. Maccaferri, A. Maris, A. Millemaggi, W. Caminati, P. G. Favero, *Chem. Phys. Lett.* **1996**, *261*, 267.
[5] S. Tang, L. Evangelisti, B. Velino, W. Caminati, *J. Chem. Phys.* **2008**, *129*, 144301.
[6] A. Maris, W. Caminati, *J. Chem. Phys.* **2003**, *118*, 1649.
[7] a) P. Ottaviani, A. Maris, W. Caminati, Y. Tatamitani, Y. Suzuki, T. Ogata, J. L. Alonso, *Chem. Phys. Lett.* **2002**, *361*, 341; b) Y. Morita, N. Ohashi, Y. Kawashima, E. Hirota, *J. Chem. Phys.* **2006**, *124*, 094301; c) A. Costantini, A. Laganà, F. Pirani, A. Maris, W. Caminati, *Lect. Notes Comput. Sci.* **2005**, *3480*, 1046; d) A. Maris, P. Ottaviani, S. Melandri, W. Caminati, A. Costantini, A. Laganà, F. Pirani, *J. Mol. Spectrosc.* **2009**, *257*, 29.
[8] B. Velino, S. Melandri, W. Caminati, *J. Phys. Chem. A* **2004**, *108*, 4224.
[9] a) L. B. Favero, B. Velino, A. Millemaggi, W. Caminati, *ChemPhysChem* **2003**, *4*, 881; b) W. Caminati, A. Millemaggi, J. L. Alonso, A. Lesarri, J. C. Lopez, S. Mata, *Chem. Phys. Lett.* **2004**, *392*, 1.
[10] a) R. Meyer, J. C. López, J. L. Alonso, S. Melandri, P. G. Favero, W. Caminati, *J. Chem. Phys.* **1999**, *111*, 7871; b) D. G. Melnik, S. Gopalakrishnan, T. A. Miller, F. C. De Lucia, *J. Chem. Phys.* **2003**, *118*, 3589.
[11] S. Melandri, J. C. López, P. G. Favero, W. Caminati, J. L. Alonso, *Chem. Phys.* **1998**, *239*, 229.
[12] a) Z. Kisiel, *J. Phys. Chem.* **1991**, *95*, 7605; Z. Kisiel, P. W. Fowler, A. C. Legon, *J. Chem. Phys.* **1991**, *95*, 2283.
[13] Z. Kisiel, "PROSPE – Programs for Rotational SPEctroscopy", available at http://info.ifpan.edu.pl/~kisiel/prospe.htm.
[14] For example, see: S. Blanco, S. Melandri, A. Maris, W. Caminati, B. Velino, Z. Kisiel, *Phys. Chem. Chem. Phys.* **2003**, *5*, 1359.
[15] Gaussian 03, Revision B.01, M. J. Frisch, G. W. Trucks, H. B. Schlegel, G. E. Scuseria, M. A. Robb, J. R. Cheeseman, J. A. Montgomery, Jr., T. Vreven, K. N. Kudin, J. C. Burant, J. M. Millam, S. S. Iyengar, J. Tomasi, V. Barone, B. Mennucci, M. Cossi, G. Scalmani, N. Rega, G. A. Petersson, H. Nakatsuji, M. Hada, M. Ehara, K. Toyota, R. Fukuda, J. Hasegawa, M. Ishida, T. Nakajima, Y. Honda, O. Kitao, H. Nakai, M. Klene, X. Li, J. E. Knox, H. P. Hratchian, J. B. Cross, C. Adamo, J. Jaramillo, R. Gomperts, R. E. Stratmann, O. Yazyev, A. J. Austin, R. Cammi, C. Pomelli, J. W. Ochterski, P. Y. Ayala, K. Morokuma, G. A. Voth, P. Salvador, J. J. Dannenberg, V. G. Zakrzewski, S. Dapprich, A. D. Daniels, M. C. Strain, O. Farkas, D. K. Malick, A. D. Rabuck, K. Raghavachari, J. B. Foresman, J. V. Ortiz, Q. Cui, A. G. Baboul, S. Clifford, J. Cioslowski, B. B. Stefanov, G. Liu, A. Liashenko, P. Piskorz, I. Komaromi, R. L. Martin, D. J. Fox, T. Keith, M. A. Al-Laham, C. Y. Peng, A. Nanayakkara, M. Challacombe, P. M. W. Gill, B. Johnson, W. Chen, M. W. Wong, C. Gonzalez, J. A. Pople, Gaussian, Inc., Pittsburgh PA, **2003**.
[16] J. K. G. Watson in *Vibrational Spectra and Structure, Vol. 6* (Ed.: J. R. Durig), Elsevier, New York, **1977**, pp. 1–89.
[17] a) H. M. Pickett, *J. Chem. Phys.* **1972**, *56*, 1715; b) H. M. Pickett, *J. Mol. Spectrosc.* **1991**, *148*, 371.
[18] J. C. López, J. L. Alonso, F. J. Lorenzo, V. M. Rayón, J. A. Sordo, *J. Chem. Phys.* **1999**, *111*, 6363.
[19] J. L. Alonso, J. C. Lopez, S. Blanco, A. Lesarri, F. J. Lorenzo, *J. Chem. Phys.* **2000**, *113*, 2760.
[20] J. Kraitchman, *Am. J. Phys.* **1953**, *21*, 17.
[21] D. J. Millen, *Can. J. Chem.* **1985**, *63*, 1477.
[22] W. G. Read, E. J. Campbell, G. Henderson, *J. Chem. Phys.* **1983**, *78*, 3501.
[23] S. E. Novick, S. J. Harris, K. C. Janda, W. Klemperer, *Can. J. Phys.* **1975**, *53*, 2007.
[24] B. Velino, S. Melandri, A. Maris, P. G. Favero, W. Caminati, *Mol. Phys.* **2002**, *98*, 1919.
[25] B. Velino, A. Millemaggi, W. Caminati, *J. Mol. Spectrosc.* **2002**, *215*, 73.
[26] M. Meyer, *J. Mol. Spectrosc.* **1979**, *76*, 266.
[27] T. J. Balle, W. H. Flygare, *Rev. Sci. Instrum.* **1981**, *52*, 33.
[28] a) J.-U. Grabow, W. Stahl, *Z. Naturforsch. A* **1990**, *45*, 1043; b) J.-U. Grabow, Ph.D. Thesis, Christian-Albrechts-Universität zu Kiel, Kiel (Germany), **1992**; c) J.-U. Grabow, W. Stahl, H. Dreizler, *Rev. Sci. Instrum.* **1996**, *67*, 4072; d) J.-U. Grabow, Habilitationsschrift, Universität Hannover, Hannover (Germany), **2004**; e) Program available at http://www.pci.uni-hannover.de/~lgpca/spectroscopy/ftmw.

Received: September 2, 2011
Published online on November 23, 2011

